Melt-rich lithosphere-asthenosphere boundary inferred from petit-spot volcanoes

Junji Yamamoto[1,2], Jun Korenaga[3], Naoto Hirano[4], and Hiroyuki Kagi[5]
[1]The Hokkaido University Museum, 8 Nishi, 10 Kita, Kita-ku, Sapporo 060-0810, Japan
[2]Institute for Geothermal Sciences, Kyoto University, Noguchibaru, Beppu 874-0903, Japan
[3]Department of Geology and Geophysics, Yale University, P.O. Box 208109, New Haven, Connecticut 06520-8109, USA
[4]Center for Northeast Asian Studies, Tohoku University, 41 Kawauchi, Aoba-ku, Sendai 980-8576, Japan
[5]Geochemical Research Center, University of Tokyo, 7-3-1 Hongo, Bunkyo-ku, Tokyo 113-0033, Japan

ABSTRACT

Young basaltic knolls have been discovered on the old oceanic lithosphere, namely petit-spot volcanoes. Based on their geochemical signatures, they have presumably originated from partial melts in the asthenosphere. However, there is no direct information on the depth provenance of petit-spot formation. Here we report new geothermobarometric data of rare mantle xenoliths discovered from petit-spot lavas exhibiting a geotherm much hotter than expected for the ca. 140 Ma seafloor on which petit-spots were formed. Such an anomalously hot geotherm indicates that melt porosity around the lithosphere-asthenosphere boundary (LAB) must be as high as a few percent. Such high melt porosity would be possible by continuous melt replenishment. Excess pressure induced by the outer-rise topography enables horizontal melt migration along the LAB and sustains a continuous melt supply to petit-spot magmatism. Given the general age-depth relationship of ocean basins, a melt-rich boundary region could also be a global feature.

INTRODUCTION

Debates on the presence of partial melts in the asthenosphere have intensified recently. The occurrences of a seismic low-velocity zone and a high electric-conductive layer in upper mantle, for example, have provided supporting evidence for partial melting in the asthenosphere (e.g., Sifré et al., 2014), which is consistent with the experimentally determined peridotite solidus in the presence of H_2O and CO_2 (Wyllie, 2012). However, recent studies suggest that partial melts are not required to explain seismic observations (Faul and Jackson, 2005; Stixrude and Lithgow-Bertelloni, 2005; Priestley and McKenzie, 2006). In order to assess the presence of the melt, petit-spot volcanism deserves attention. Petit-spot volcanoes are tiny seamounts erupting off the fore-bulge of the downgoing oceanic plate (Hirano et al., 2004, 2006). Petit-spots have been successively discovered at many sites in the world (e.g., Hirano et al., 2006, 2008, 2013), suggesting that petit-spot magmatism is ubiquitous at areas of plate flexure. Because of their isotopic similarities to mid-ocean-ridge basalts, petit-spot magmas are likely to be derived from partial melts in the ambient asthenosphere (Hirano et al., 2006). Therefore, petit-spots are invaluable samples of asthenospheric partial melts beneath a mature oceanic lithosphere; a good understanding of how petit-spots actually form can provide entirely new insight into the physical state of the normal upper mantle.

So far, about a dozen mantle xenoliths have been recovered from petit-spot lavas (Yamamoto et al., 2009). The occurrence of the mantle xenoliths provides essential information on the host magma, such as the origin and ascent rate of the magma. In addition, these xenoliths can constrain how the oceanic lithosphere is affected by petit-spot formation. As long-standing volcanism at an old oceanic plate is expected to affect the geotherm, the thermal structure of the oceanic plate deduced from the mantle xenoliths could potentially test the occurrence of melt at the base of the lithosphere.

THERMAL STRUCTURE OF THE OCEANIC LITHOSPHERE

We used five xenoliths recovered from petit-spot basalts erupting on subducting Pacific Plate off the Japan Trench (Fig. DR1 in the GSA Data Repository[1]). To infer the thermal structure of the oceanic plate from which these xenoliths are supposed to have originated, we need geothermobarometric data of the mantle xenoliths. The temperature was estimated using the two-pyroxene thermometer proposed by Wells (1977). The range of temperature is 771–1129 °C (Tables DR1 and DR2 in the Data Repository). Regarding the pressure, we conducted a thorough investigation of the depth provenance of the xenoliths based on pressure information recorded in the mantle xenoliths such as thermodynamic geobarometry, mineralogy, and the residual pressure of fluid inclusions and their stability conditions. We summarize the essence of the investigation here. The xenoliths are spinel peridotites, which are stable in mantle at 1.0–2.2 GPa (O'Neill, 1981; Borghini et al., 2010). In addition, there are abundant CO_2 inclusions in the xenoliths. Taking the stability conditions of CO_2 fluid in olivine into consideration (Koziol and Newton, 1998), the present spinel peridotites should be derived from the pressure-temperature (*P-T*) conditions depicted by a shaded area in Figure 1.

There is geobarometry based on residual pressure of fluid inclusions, which can be applied to mantle xenoliths (e.g., Miller and Richter, 1982). The estimated pressure and temperature are shown in Figure 1 (see the Data Repository for data and analytical procedures). There is considerable validity to the pressure estimated by the fluid inclusion geobarometry because the *P-T* values are well supported by the stability conditions of both aluminum-bearing minerals and CO_2 fluid in olivine. The estimated pressures have a positive correlation with the temperatures. The most plausible explanation for the correlation is that they reflect the geotherm beneath the sampling sites, but the geothermobarometric data of these mantle xenoliths imply a very hot geotherm corresponding to young (ca. 18 Ma) oceanic lithosphere (Fig. 1). Such a geotherm must be a localized feature, restricted to the vicinity of these petit-spots; if it represented a regional geotherm, an isostatic adjustment would have raised the seafloor by as much as ~2 km (Turcotte and Schubert, 2002). This view of a highly localized hot geotherm is also consistent with the spotty distribution of anomalously high heat-flow data reported from this region (Yamano et al., 2008).

GENERATION MECHANISM OF PETIT-SPOT MAGMA

The existence of localized thermal anomalies in the old oceanic lithosphere thus appears to be feasible, and as discussed below, two lines of reasoning suggest that such thermal anomalies may have profound implications for the origin of petit-spots as well as the nature of the lithosphere-asthenosphere boundary.

First, the amount of excess heat required to generate the thermal anomaly may be estimated as

$$\Delta E = C_p \Delta T \rho_m HA, \quad (1)$$

[1]GSA Data Repository item 2014342, supplementary information about the samples and the accuracy of the geobarometry, is available online at www.geosociety.org/pubs/ft2014.htm, or on request from editing@geosociety.org or Documents Secretary, GSA, P.O. Box 9140, Boulder, CO 80301, USA.

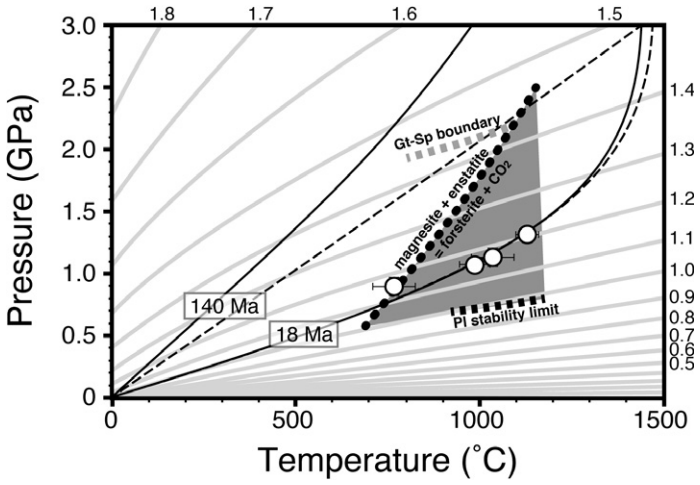

Figure 1. Pressure-temperature (*P-T*) diagram for the CO_2 system (Pitzer and Sterner, 1994). Gray contours represent density in g cm^{-3} (i.e., isochors). The pressure at which mantle xenoliths were trapped by host magma can be estimated from intersections of isochors with two-pyroxene temperatures (open circles). The *P-T* data are provided in Table DR3 (see footnote 1). Error bars for pressure are almost within the size of symbols. Also shown are geotherms for 18 Ma and 140 Ma oceanic lithosphere, using half-space cooling (solid) and the plate model GDH1 (Stein and Stein, 1992) (dashed). The seafloor age of 140 Ma is appropriate for Yukawa and Kaiko knolls, whereas the age of 18 Ma is chosen to best fit the xenolith data. Dotted line is the reaction (phase boundary): magnesite + enstatite = forsterite + CO_2 (Koziol and Newton, 1998). The CO_2 is able to coexist with forsterite at the region on the right hand of the dotted line. Gray and black heavy dashed lines denote the garnet-spinel (Gt-Sp) boundary (O'Neill, 1981) and upper-limit pressure for the plagioclase (Pl) stability field (Borghini et al., 2010), respectively. Thus the spinel peridotites with CO_2 inclusions in olivine should exist at the *P-T* conditions depicted by a shaded area.

where C_p is the specific heat for mantle peridotite (1 kJ kg^{-1} K^{-1}), ΔT is the average temperature excess (~300 K; average temperature difference between the 18 Ma and 140 Ma geotherm), ρ_m is the mantle density (3300 kg m^{-3}), H is the thickness of the lithosphere (~100 km), and A is the cross-sectional area of an affected region. For an area of 1 km^2, for example, the excess heat would be ~10^{20} J, equivalent to the latent heat of solidification released from ~75 km^3 of melt. A typical petit-spot is only ~50 m high, with a footprint of 1 km^2 (Hirano et al., 2006), so the melt volume required for the excess heat could be greater than the erupted volume by more than three orders of magnitude. This inference is admittedly crude, being sensitive to the assumed cross-sectional area. Pyroxenes in two mantle xenoliths, however, do not show notable zoning, and given the diffusion rate of ~10^{-20} m^2 s^{-1} for the inter-diffusion of elements relevant for geothermometry (Zhang et al., 2010), heating must have continued for at least 1 m.y. to achieve grain-scale chemical re-equilibration, during which a thermal anomaly could have spread for a few kilometers. The cross-sectional area thus must be greater than a few square kilometers. Even though petit-spots appear to be volumetrically trivial, therefore, the associated thermal anomalies in the lithosphere suggest that these surface expressions may well be just "the tip of the iceberg."

Second, the formation of petit-spots requires melt migration through thick oceanic lithosphere, and a quantitative consideration suggests a rather specific circumstance, beyond a favorable stress state caused by nearby plate bending (Hirano et al., 2006). To avoid freezing within the lithosphere, melt has to travel sufficiently fast, or the Peclet number must be substantially greater than unity (Turcotte and Schubert, 2002):

$$Pe = \frac{vh}{\kappa} \gg 1, \tag{2}$$

where v is vertical melt velocity, h is a channel width, and κ is thermal diffusivity (10^{-6} m^2 s^{-1}). A primary rate-limiting factor for melt ascent is the supply rate through the base of the lithosphere, which may be seen in the following mass conservation equation:

$$vh \sim u\phi\delta_c \sim \frac{k_\phi}{\mu}\frac{dp}{dx}\delta_c, \tag{3}$$

where u is horizontal melt velocity, ϕ is melt porosity in the asthenosphere, δ_c is compaction length, k_ϕ is permeability, μ is melt viscosity (10 Pa·s), and dp/dx is the horizontal pressure gradient. The first term is vertical melt flux, and the second term is horizontal melt flux, which is expanded by Darcy's law in the last expression. Partial melt in the asthenosphere would migrate upward by its own buoyancy and pool beneath the lithosphere. Though complete melt segregation is unlikely at low porosities, we can still expect a relatively melt-rich region due to compaction, the vertical scale of which can be estimated by the compaction length (McKenzie, 1984; Sparks and Parmentier, 1991). Horizontal melt migration is possible with a nonzero horizontal pressure gradient, and in the case of petit-spot magmatism, the outer-rise topography is the most important source for such excess pressure (Fig. 2), i.e.,

$$\frac{dp}{dx} \sim \frac{(\rho_m - \rho_w)g\Delta d}{L}, \tag{4}$$

where ρ_w is the density of sea water (1000 kg m^{-3}), g is gravitational acceleration (9.8 m s^{-2}), Δd is the excess topography of the outer rise (~800 m),

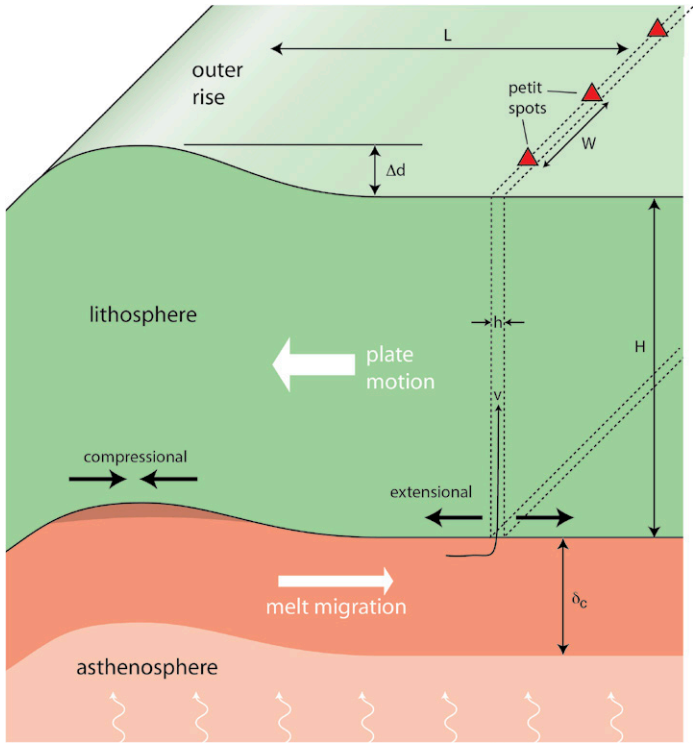

Figure 2. Schematic illustration of a fluid dynamical model for petit-spot formation. Partial melts in asthenosphere are slowly migrating upward and ponding beneath oceanic lithosphere. The length scale of the ponded region is given by compaction length δ_c. Ponded melts, except for those in the lithospheric trap (dark shade), migrate horizontally due to the topographic head of the outer rise. Horizontal pressure gradient is controlled by the excess topography of Δd and the lateral length scale of L. The product of vertical melt velocity v and channel width h is constrained by this horizontal melt transport, though vertical melt velocity can increase by focusing melt transport so that petit-spot formation is spatially localized, at an interval of W. The illustration is not drawn to scale; in particular, note that $H >> \delta_c > \Delta d$.

and L is the horizontal spatial scale (~600 km). Matrix shear associated with the bending of oceanic lithosphere also results in a horizontal pressure gradient (McKenzie, 1984), which adds to the above pressure gradient. The pressure gradient due to bending, however, is on the order of $\eta V / L^2$, where η is matrix viscosity and V is plate velocity, being considerably smaller than the pressure gradient due to the outer-rise topography. At any rate, without continuous melt delivery from the asthenosphere, melt migration through the lithosphere would resemble the propagation of a buoyancy-driven melt-filled crack with constant volume, the thermal fate of which depends strongly on initial melt volume (Spence and Turcotte, 1990). Our formulation above may be regarded as a continuum approximation for discrete crack propagation. As already suggested (Hirano et al., 2006), we assume that vertical melt transport becomes prominent when the stress state at the base of lithosphere becomes extensional, i.e., far away from the outer rise.

Permeability is a function of porosity and grain size (Fig. 3A), and the compaction length is a function of permeability, melt viscosity, and matrix viscosity. Using values appropriate for asthenospheric mantle, the compaction length is found to be on the order of ~10 m to a few kilometers (Fig. 3B). By combining Equations 2–4, the Peclet number can be expressed as a function of porosity, and if melt migration is entirely two-dimensional (2-D; i.e., no variation along the horizontal axis perpendicular to plate motion), melt porosity has to be much higher than 10% to make the Peclet number greater than unity (see 2-D line in Fig. 3C). This estimate is insensitive to the channel width h, because the horizontal melt delivery rate constrains the total product of the channel width and vertical melt velocity, vh (Equation 3). It is unlikely, however, that melt migration would remain 2-D, and any 3-D focusing can raise the Peclet number. If such 3-D effects eventually result in the average spacing, W, between petit-spots, the Peclet number would increase by a factor of W/h; for h of 100 m and W of 100 km, for example, surface eruption would become possible even with the porosity of ~3% (Fig. 3C). Moreover, from the very fact that mantle xenoliths (with a size of ~1 cm) were collected from petit-spots, vertical melt velocity must have become as high as ~1 cm s^{-1} at some point in petit-spot evolution (Rutherford, 2008), which corresponds to the Peclet number of 10^4–10^6 with a channel width of 1–100 m. For reasonable ranges of channel width (1–100 m) and petit-spot spacing (10–1000 km), the focusing factor W/h can be as high as 10^6, so it is possible to achieve such a high Peclet number if melt porosity is as high as a few percent (Fig. 3C); because of uncertainty in grain size and matrix viscosity, we cannot be more specific about required melt porosity, but it is difficult to achieve Peclet number of 10^4 with melt porosity less than 1%. Also note that, for melts to flow seaward from the outer rise, the compaction length has to be greater than the outer rise excess topography (Fig. 2), which is possible only with high porosities (Fig. 3B); otherwise, overpressured melts would be entirely trapped within the flexed base of the lithosphere.

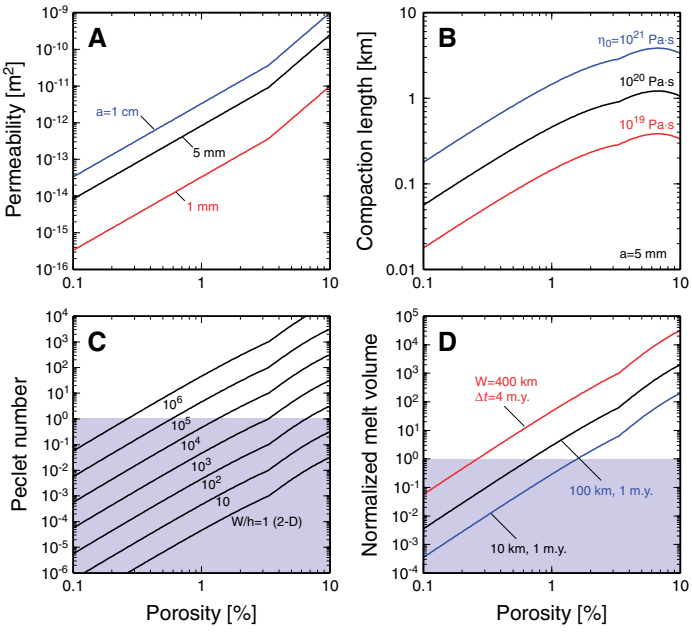

Figure 3. Theoretical results for melt migration. A: Permeability of partially molten asthenosphere as a function of porosity (McKenzie, 1989). Three grain sizes are used to cover a likely range for mantle olivine. B: Compaction length as a function of porosity, calculated as $\delta_c = \sqrt{k_\phi \eta / \mu}$, where k_ϕ is permeability, $\eta = \eta_0 \exp(-45\phi)$ (Kelemen et al., 1997), η_0 is reference matrix viscosity, ϕ is melt porosity in the asthenosphere, and μ is melt viscosity. The range of reference viscosity, 10^{19}–10^{21} Pa·s, covers the uncertainty of mantle viscosity under asthenospheric conditions (Korenaga and Karato, 2008). C: Peclet number based on Equations 2–4 (grain size of 5 mm and η_0 of 10^{20} Pa·s are assumed here). Different curves correspond to different degrees of three-dimensional focusing W/h, where W is average spacing between petit-spots and h is channel width (2-D—two-dimensional). D: Total melt volume delivered to a petit-spot with a spacing of W during a period of Δt (i.e., $u\phi W\Delta t$, where u is horizontal melt velocity), normalized by the typical volume of surface expression (Hirano et al., 2006) (~5 × 10^7 m^3).

A likely scenario for petit-spot formation would therefore start with nearly complete failures of vertical melt migration by initially 2-D flow and gradually shift to more successful melt ascents by 3-D focusing. During this process, a column of lithosphere beneath a petit-spot would be heated up, resulting in an anomalous geotherm. Using Equation 3, we can estimate the volume of melt delivered per petit-spot by assuming the petit-spot spacing and the duration of melt delivery (Fig. 3D). For a plate velocity of 10 cm yr^{-1} and one petit-spot per area of 100 × 100 km, the total melt volume delivered from the asthenosphere would be greater than that of the surface expression by 2–3 orders of magnitude for melt porosity of a few percent (Fig. 3D). The volcanic construct of a petit-spot thus represents only a small fraction of the total melt volume required to make surface eruption possible.

DISCUSSION AND CONCLUSIONS

A broad agreement between the two different estimates on the total melt volume involved, one based on excess heat anomaly and the other based on the dynamics of melt transport, is encouraging, but our preferred melt porosity (>1%) may be problematic; with volatile contents similar to the sources of mid-ocean-ridge basalt, only very small amounts of melt (<0.1%) are predicted to exist under asthenospheric conditions (Hirschmann, 2010). By vertical migration, however, melt can pond beneath the lithosphere, where melt porosity can be locally high. Indeed, this process is already assumed in our conceptual model by the use of compaction length (Fig. 2). The presence of the seismic G discontinuity, which is the stratum in mantle as detected by changes in seismic wave velocity (Kawakatsu et al., 2009; Revenaugh and Jordan, 1991; Gaherty et al., 1996), often associated with the lithosphere-asthenosphere boundary, requires a sharp and large velocity drop, which could be explained by such melt ponding. Without continuous replenishment, ponded melt would be frozen by a growing lithosphere (Hirschmann, 2010), but oceanic lithosphere does not simply grow, as inferred from the age-depth relationship of global seafloor. It has long been known that simple half-space cooling cannot explain the subsidence of the seafloor when the age of the seafloor exceeds ca. 70 Ma (Parsons and Sclater, 1977) (Fig. 1), clearly indicating that oceanic lithosphere is subject to excess heat supply from below. A recent statistical analysis of global age-depth data (Korenaga and Korenaga, 2008) shows that a majority of seafloor is affected by the formation of hotspots and oceanic plateaus, much broader areas than implied by the spatial extent of those volcanic features. The presence of petit-spots may reflect a regional feature specific to the northwestern Pacific (Obayashi et al., 2006), but the above considerations suggest that a thin, melt-rich layer could potentially exist at many other places beneath oceanic lithosphere;

recent geophysical studies (Schmerr, 2012; Naif et al., 2013) appear to be consistent with this view. Because of a limited number of so-far discovered petit-spots, it is difficult to judge the robustness of this inference, but the anomalous geotherm revealed by these rare mantle xenoliths provides a unique perspective to the ongoing debate on the nature of the lithosphere-asthenosphere boundary, through the fluid dynamics of petit-spot formation.

ACKNOWLEDGMENTS

Two anonymous reviewers provided thoughtful comments that improved the manuscript. This work has been funded by a Toray Science and Technology Grant (no. 11-5208) and Grants-in-Aid for Scientific Research (nos. 23654160, 25287139) from the Japan Society for the Promotion of Science. Korenaga was supported in part by a visiting professorship at Kyoto University.

REFERENCES CITED

Borghini, G., Fumagalli, P., and Rampone, E., 2010, The stability of plagioclase in the upper mantle: Subsolidus experiments on fertile and depleted lherzolite: Journal of Petrology, v. 51, p. 229–254, doi:10.1093/petrology/egp079.

Faul, U.H., and Jackson, I., 2005, The seismological signature of temperature and grain size variations in the upper mantle: Earth and Planetary Science Letters, v. 234, p. 119–134, doi:10.1016/j.epsl.2005.02.008.

Gaherty, J.B., Jordan, T.H., and Gee, L.S., 1996, Seismic structure of the upper mantle in a central Pacific corridor: Journal of Geophysical Research, v. 101, p. 22,291–22,309, doi:10.1029/96JB01882.

Hirano, N., Yamamoto, J., Kagi, H., and Ishii, T., 2004, Young olivine xenocryst-bearing alkali-basalt from the oceanward slope of the Japan Trench: Contributions to Mineralogy and Petrology, v. 148, p. 47–54, doi:10.1007/s00410-004-0593-z.

Hirano, N., et al., 2006, Volcanism in response to plate flexure: Science, v. 313, p. 1426–1428, doi:10.1126/science.1128235.

Hirano, N., Koppers, A.A.P., Takahashi, A., Fujiwara, T., and Nakanishi, M., 2008, Seamounts, knolls and petit-spot monogenetic volcanoes on the subducting Pacific Plate: Basin Research, v. 20, p. 543–553, doi:10.1111/j.1365-2117.2008.00363.x.

Hirano, N., Machida, S., Abe, N., Morishita, T., Tamura, A., and Arai, S., 2013, Petit-spot lava fields off the central Chile trench induced by plate flexure: Geochemical Journal, v. 47, p. 249–257, doi:10.2343/geochemj.2.0227.

Hirschmann, M.M., 2010, Partial melt in the oceanic low velocity zone: Physics of the Earth and Planetary Interiors, v. 179, p. 60–71, doi:10.1016/j.pepi.2009.12.003.

Kawakatsu, H., Kumar, P., Takei, Y., Shinohara, M., Kanazawa, T., Araki, E., and Suyehiro, K., 2009, Seismic evidence for sharp lithosphere-asthenosphere boundaries of oceanic plates: Science, v. 324, p. 499–502.

Kelemen, P.B., Girth, G., Shimizu, N., Spiegelman, M., and Dick, H.J.B., 1997, A review of melt migration processes in the adiabatically upwelling mantle beneath oceanic spreading ridges: Philosophical Transaction of the Royal Society of London, ser. A, v. 355, p. 283–318, doi:10.1098/rsta.1997.0010.

Korenaga, J., and Karato, S., 2008, A new analysis of experimental data on olivine rheology: Journal of Geophysical Research, v.113, B02403 doi:101029/2007JB005100.

Korenaga, T., and Korenaga, J., 2008, Subsidence of normal oceanic lithosphere apparent thermal expansivity and seafloor flattening: Earth and Planetary Science Letters, v. 268, p. 41–51, doi:10.1016/j.epsl.2007.12.022.

Koziol, A.M., and Newton, R.C., 1998, Experimental determination of the reaction: magnesite + enstatite = forsterite + CO_2 in the ranges 6–25 kbar and 700–1100°C: The American Mineralogist, v. 83, p. 213–219.

McKenzie, D., 1984, The generation and compaction of partially molten rock: Journal of Petrology, v. 25, p. 713–765, doi:10.1093/petrology/25.3.713.

McKenzie, D., 1989, Some remarks on the movement of small melt fractions in the mantle: Earth and Planetary Science Letters, v. 95, p. 53–72, doi:10.1016/0012-821X(89)90167-2.

Miller, C., and Richter, W., 1982, Solid and fluid phases in lherzolite and pyroxenite inclusions from the Hoggar, central Sahara: Geochemical Journal, v. 16, p. 263–277, doi:10.2343/geochemj.16.263.

Naif, S., Key, K., Constable, S., and Evans, R.L., 2013, Melt-rich channel observed at the lithosphere-asthenosphere boundary: Nature, v. 495, p. 356–359, doi:10.1038/nature11939.

Obayashi, M., Sugioka, H., Yoshimitsu, J., and Fukao, Y., 2006, High temperature anomalies oceanward of subducting slabs at the 410-km discontinuity: Earth and Planetary Science Letters, v. 243, p. 149–158, doi:10.1016/j.epsl.2005.12.032.

O'Neill, H.St.C., 1981, The transition between spinel lherzolite and garnet lherzolite and its use as a geobarometer: Contributions to Mineralogy and Petrology, v. 77, p. 185–194, doi:10.1007/BF00636522.

Parsons, B., and Sclater, J.G., 1977, An analysis of the variation of ocean floor bathymetry and heat flow with age: Journal of Geophysical Research, v. 82, p. 803–827, doi:10.1029/JB082i005p00803.

Pitzer, K.S., and Sterner, S.M., 1994, Equations of state valid continuously from zero to extreme pressures for H_2O and CO_2: The Journal of Chemical Physics, v. 101, p. 3111–3116, doi:10.1063/1.467624.

Priestley, K., and McKenzie, D., 2006, The thermal structure of the lithosphere from shear wave velocities: Earth and Planetary Science Letters, v. 244, p. 285–301, doi:10.1016/j.epsl.2006.01.008.

Revenaugh, J.S., and Jordan, T.H., 1991, Mantle layering from *ScS* reverberations: 3. The upper mantle: Journal of Geophysical Research, v. 96, p. 19,781–19,810, doi:10.1029/91JB01487.

Rutherford, M.J., 2008, Magma ascent rates: Reviews in Mineralogy and Geochemistry, v. 69, p. 241–271, doi:10.2138/rmg.2008.69.7.

Schmerr, N., 2012, The Gutenberg discontinuity: Melt at the lithosphere-asthenosphere boundary: Science, v. 335, p. 1480–1483, doi:10.1126/science.1215433.

Sifré, D., Gardés, E., Massuyeau, M., Hashim, L., Hier-Majumder, S., and Gaillard, F., 2014, Electrical conductivity during incipient melting in the oceanic low-velocity zone: Nature, v. 509, p. 81–85, doi:10.1038/nature13245.

Sparks, D.W., and Parmentier, E.M., 1991, Melt extraction from the mantle beneath spreading centers: Earth and Planetary Science Letters, v. 105, p. 368–377, doi:10.1016/0012-821X(91)90178-K.

Spence, D.A., and Turcotte, D.L., 1990, Buoyancy-driven magma fracture: A mechanism for ascent through the lithosphere and the emplacement of diamonds: Journal of Geophysical Research, v. 95, p. 5133–5139, doi:10.1029/JB095iB04p05133.

Stein, C.A., and Stein, S., 1992, A model for the global variation in oceanic depth and heat flow with lithospheric age: Nature, v. 359, p. 123–129, doi:10.1038/359123a0.

Stixrude, L., and Lithgow-Bertelloni, C., 2005, Mineralogy and elasticity of the oceanic upper mantle: Origin of the low-velocity zone: Journal of Geophysical Research, v. 110, B03204, doi:10.1029/2004JB002965.

Turcotte, D.L., and Schubert, G., 2002, Geodynamics, 2nd Edition: Cambridge, UK, Cambridge University Press, 472 p.

Wells, P.R.A., 1977, Pyroxene thermometry in simple and complex systems: Contributions to Mineralogy and Petrology, v. 62, p. 129–139, doi:10.1007/BF00372872.

Wyllie, P.J., 2012, Solidus curves mantle plumes and magma generation beneath Hawaii: Journal of Geophysical Research, v. 93, p. 4171–4181, doi:10.1029/JB093iB05p04171.

Yamamoto, J., Hirano, N., Abe, N., and Hanyu, T., 2009, Noble gas isotopic compositions of mantle xenoliths from northwestern Pacific lithosphere: Chemical Geology, v. 268, p. 313–323, doi:10.1016/j.chemgeo.2009.09.009.

Yamano, M., Kinoshita, M., and Goto, S., 2008, High heat flow anomalies on an old oceanic plate observed seaward of the Japan Trench: International Journal of Earth Sciences, v. 97, p. 345–352, doi:10.1007/s00531-007-0280-1.

Zhang, X., Ganguly, J., and Ito, M., 2010, Ca-Mg diffusion in diopside: Tracer and chemical inter-diffusion coefficients: Contributions to Mineralogy and Petrology, v. 159, p. 175–186, doi:10.1007/s00410-009-0422-5.

Manuscript received 31 May 2014
Revised manuscript received 7 August 2014
Manuscript accepted 9 August 2014

Printed in USA